

Research Article

Assessment of Fractional and Integer Order Models of Induction Motor Using MATLAB/Simulink

Girma Kassa Alitasb 

Department of Electrical and Computer Engineering, Debre Markos University, Debre Markos, Ethiopia

Correspondence should be addressed to Girma Kassa Alitasb; girma_kassa@dmu.edu.et

Received 2 December 2023; Revised 15 March 2024; Accepted 20 March 2024; Published 12 April 2024

Academic Editor: Franco Ramírez

Copyright © 2024 Girma Kassa Alitasb. This is an open access article distributed under the Creative Commons Attribution License, which permits unrestricted use, distribution, and reproduction in any medium, provided the original work is properly cited.

The definition of derivatives and integrals of any real or complex order can be found in fractional calculus, which is an extension of ordinary calculus. Many real-world processes might be more accurately modeled by these fractional calculi. Flexibility and nonlocality are the two fundamental benefits of fractional derivatives. These derivatives, which are of fractional order, are more flexible than classical derivatives in how they might approach real data. Due to its applications in numerous domains, the fractional order model has grown in significance and popularity. The simulation results have been performed for three squirrel cage induction motors which have different parameter values. To perform fractional order calculus, the Fractional Order Modeling and Control (FOMCOM) toolbox has been added to MATLAB. To determine the value of the order of differentiation (α) that best represents the induction motor, speed and torque simulations for several orders of differentiation (α) were performed. According to the results of the speed and torque simulation, an integer order ($\alpha = 1$) model is the optimal representation of the induction motor. The main goal of this paper is to investigate which model, either integer or fractional order model, best represents an induction motor.

1. Introduction

In control of dynamic systems, fractional integrals and derivatives are used when a fractional differential equation is used to describe the controlled system or the controller [1]. The advantages of applying fractional order calculus in several scientific fields, such as modeling and automated control, made it more widely used in recent years. Indeed, such an increase in attention is associated with the development of computer algebra systems (CAS), including MATLAB and Mathematica, as well as the availability of much more potent and effective computational methods made available by technological improvement [2].

Latest studies provide evidence in favor of the use of fractional order calculus for more precise modeling and control. Particularly, difficult mathematics and physical issues used fractional order calculus [3].

Fractional (noninteger order) systems can be considered an extension of integer order systems. The fractional order operator, aD_t^α , where a and t are the operation's limit and $\alpha \in R$, is defined as [4]

$$aD_t^\alpha = \begin{cases} \frac{d^\alpha}{dt^\alpha}, & \alpha > 0, \\ 1, & \alpha = 0, \\ \int_a^t (d\tau)^{-\alpha}, & \alpha < 0. \end{cases} \quad (1)$$

Laplace transform is a crucial technique for modeling dynamic systems. There are several ways to define the fractional operator. The key definitions of fractional order derivatives are provided in the section below [1, 4–8].

(1) The Riemann-Liouville fractional order derivative definition is as follows

$$aD_t^\alpha f(t) = \frac{1}{\Gamma(m-\alpha)} \frac{d^m}{dt^m} \int_a^t (t-\tau)^{m-\alpha-1} f(\tau) d\tau, \quad (2)$$

where $m-1 < \alpha \leq m \in N$, $\alpha \in R$, and α represent the order of differentiation of function $f(t)$. $\Gamma(\cdot)$ is the gamma function.

Laplace transform of causal system based on the Riemann-Liouville fractional order differentiation definition becomes

$$\mathcal{L}[{}^0D_t^\alpha f(t)] = s^\alpha F(s) - \sum_{k=0}^{n-1} s^k {}^0D_t^{\alpha-k-1} f(0), \quad (3)$$

where $f(0)$ are the initial conditions and $n-1 < \alpha \leq n \in N$.

(2) The Caputo fractional order derivative definition is as follows

$${}_aD_t^\alpha f(t) = \frac{1}{\Gamma(m-\alpha)} \int_a^t f^{(m)}(\tau) (t-\tau)^{m-\alpha-1} d\tau, \quad (4)$$

where $m-1 < \alpha \leq m \in N$, $\alpha \in R$, and α represent the order of differentiation of function $f(t)$. For a causal system, the Laplace transform based on the Caputo fractional order differentiation definition becomes

$$\mathcal{L}[{}^0D_t^\alpha f(t)] = s^\alpha F(s) - \sum_{k=0}^{n-1} s^{\alpha-k-1} f^{(k)}(0), \quad (5)$$

where $n-1 < \alpha \leq n \in N$.

$$\begin{aligned} \Gamma(x) &= \int_0^\infty t^{x-1} e^{-t} dt, \\ \Gamma(x) &= (x-1)!. \end{aligned} \quad (6)$$

(3) The Grünwald-Letnikov fractional order derivative definition is as follows

$${}_aD_t^\alpha f(t) = \lim_{h \rightarrow 0} \frac{1}{h^\alpha} \sum_{j=0}^{\lfloor (t-a)/h \rfloor} (-1)^j \binom{\alpha}{j} f(t-jh), \quad (7)$$

where $\lfloor \cdot \rfloor$ represents the integer part and h represents step size.

For a causal system, the Laplace transform based on the Grünwald-Letnikov fractional order differentiation definition becomes

$$\begin{aligned} \mathcal{L}[{}_0D_t^\alpha f(t)] &= s^\alpha F(s), \\ \binom{\alpha}{j} &= \frac{\alpha!}{j!(\alpha-j)!} = \frac{\Gamma(\alpha+1)}{\Gamma(j+1)\Gamma(\alpha-j+1)}. \end{aligned} \quad (8)$$

Fractional order differential equations can be used to model both SISO and MIMO systems. A fractional differential equation of the form can be used to describe a generic linear time-invariant fractional order system [4].

$$\begin{aligned} &a_n D_t^{\alpha_n} y(t) + a_{n-1} D_t^{\alpha_{n-1}} y(t) + \dots + a_0 D_t^{\alpha_0} y(t) \\ &= b_m D_t^{\beta_m} u(t) + b_{m-1} D_t^{\beta_{m-1}} u(t) + \dots + b_0 D_t^{\beta_0} u(t). \end{aligned} \quad (9)$$

The subsequent form describes the transfer function for incommensurate real orders.

$$G(S) = \frac{b_m S^{\beta_m} + \dots + b_1 S^{\beta_1} + b_0 S^{\beta_0}}{a_n S^{\alpha_n} + \dots + a_1 S^{\alpha_1} + a_0 S^{\alpha_0}} = \frac{Q(S^{\beta_k})}{P(S^{\alpha_k})}. \quad (10)$$

Equation (10) has the following form in the frequency domain:

$$G(j\omega) = \frac{b_m (j\omega)^{\beta_m} + \dots + b_1 (j\omega)^{\beta_1} + b_0 (j\omega)^{\beta_0}}{a_n (j\omega)^{\alpha_n} + \dots + a_1 (j\omega)^{\alpha_1} + a_0 (j\omega)^{\alpha_0}} = \frac{Q((j\omega)^{\beta_k})}{P((j\omega)^{\alpha_k})}, \quad (11)$$

where a_k ($k=0, 1, 2, 3, \dots, n$) and b_k ($k=0, 1, 2, \dots, m$) are constants and α_k ($k=0, 1, 2, \dots, n$) and β_k ($k=0, 1, 2, \dots, m$) are arbitrary numbers. Equation (10) for the incommensurate order system can alternatively be stated by the multivalued transfer function in commensurate form.

$$H(S) = \frac{b_m S^{m/\nu} + \dots + b_1 S^{1/\nu} + b_0}{a_n S^{n/\nu} + \dots + a_1 S^{1/\nu} + a_0}, \quad \nu > 1. \quad (12)$$

The following state space model can also be used to characterize the linear time-invariant fractional order systems.

$$\left. \begin{aligned} {}^0D_t^q x(t) &= Ax(t) + Bu(t) \\ y(t) &= Cx(t) + Du(t) \end{aligned} \right\}, \quad (13)$$

where $x \in R^n$, $u \in R^r$, and $y \in R^p$ are the state, input, and output vectors of the system and $A \in R^{n \times n}$, $B \in R^{n \times r}$, $C \in R^{p \times n}$, $D \in R^{p \times r}$, and $q = [q_1, q_2, q_3, \dots, q_n]^T$ are the fractional orders. If $q_1 = q_2 = \dots = q_n \equiv \alpha$, the system described by Equation (13) is a commensurate order system; otherwise, it is an incommensurate order system.

MIMO systems with fractional orders can be represented using the state-space model.

$$G(S) = C(S^q I - A)^{-1} B + D. \quad (14)$$

Nonlinear fractional order system has the form [3]

$$\begin{aligned} {}^0D_t^{q_i} x_i(t) &= f_i(x_1(t), x_2(t), \dots, x_n(t), t), \\ x_i(0) &= c_i, \quad i = 1, 2, \dots, n, \end{aligned} \quad (15)$$

where c_i represents the initial conditions.

$$D^q X = f(X), \quad (16)$$

where $q = [q_1, q_2, q_3, \dots, q_n]^T$ for $0 < q_i < 2$, ($i = 1, 2, 3, \dots, n$), and $X \in R^n$.

The speed at which the induction motor rotates is nearly equal to the synchronous speed, but not quite. Rotor speed is about equal to synchronous speed when there is no load. Thus, the induction motor's no-load speed is dependent on the number of poles and supply frequency [9].

As the power source for fans, pumps, and compressors, three-phase squirrel cage-type induction motors with capacities ranging from several kilowatts to hundreds of kilowatts are often used in industrial applications. Fractional order differential equations are more suited to describing systems in the real world. In comparison to traditional (integer) order-modeled systems, systems modeled with fractional orders provide more precise modeling and efficient control capabilities. As a result, when compared to a traditional ordered system, accurate data can be acquired from fractional order models. The main goal of this paper is to investigate which model either integer or fractional order model best represents an induction motor.

The rest of this paper is divided into the following sections. Section 2 introduces toolboxes added to MATLAB for investigating fractional order systems; Section 3 presents a dynamic D-Q model of induction motor; Section 4 covers results and analysis, and finally, Section 5 presents the conclusion.

2. Toolboxes Added to MATLAB for Investigating Fractional Order Systems

The need for numerical methods for fractional calculus computation to model fractional order systems has grown in recent years as fractional calculus is utilized widely across a variety of academic areas. The question of which tool is best for a given application comes up from time to time [10].

2.1. @fotf. Xue created the @fotf (fractional order transfer function) toolbox for modeling and control of fractional order systems. The majority of features here are extensions of built-in functions in MATLAB. Overload programming is used to enable the associated operations of the built-in MATLAB features to handle fractional order models. However, the graphing functionality was lost due to overloading of related operations. Time delay is supported in the transfer function via the @fotf toolbox. MIMO systems cannot be straightforwardly simulated since direct support for transfer function matrices is not provided. The accuracy of @fotf is affected by the sample time, which is a drawback [11].

2.2. Ninteger. The ninteger (noninteger) control toolbox for MATLAB is a set of tools for creating and evaluating fractional order controllers. In this toolbox, integer order transfer functions are used to approximate the fractional order integrator/differentiator. Additionally, it offers Simulink blocks, such as the "nid" and "nipid" blocks, that contain the relevant functions. MATLAB 2013a and subsequent versions have an issue with the integer toolbox. Because of the overload adjustment of the MATLAB built-in function "isinteger()," it contradicts with several built-in functions without further modification [12, 13].

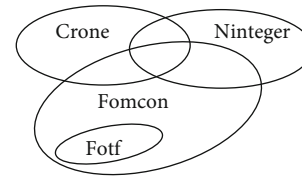


FIGURE 1: Relation between FOMCON and other fractional MATLAB toolboxes [1].

2.3. CRONE. The CRONE toolbox, created by the CRONE team since the 1990s, is a MATLAB toolbox devoted to fractional derivative fields. It changed from the initial scripted version to the present object-oriented version. The CRONE toolbox's ability to implement some of the approaches for MIMO fractional transfer functions is a useful feature. One limitation of the CRONE toolbox is that it is impossible to add delay time in the resulting fractional order transfer function [14].

2.4. FOMCON. Tepljakov created the FOMCON (Fractional Order Modeling and Control) toolbox [3]. The algorithms in @fotf, ninteger, and CRONE are used in its kernel. It combines the key features of the three toolboxes and constructs a graphical user interface, with the goal of extending traditional control strategies for fractional controller designs. Figure 1 shows the relationship between FOMCON and the three toolboxes. Because it combines the main features of the @fotf, ninteger, and CRONE toolboxes, the FOMCON MATLAB toolbox is employed in this study.

As shown in Figure 2, the FOMCON toolbox contains continuous fractional linear time-invariant transfer function, discrete fractional linear time-invariant transfer function, continuous and discrete fractional PID controllers, fractional derivative and integrator, etc. block sets to use Simulink.

3. Model of Three-Phase Induction Motor

Mathematical modeling essentially entails creating a framework, frequently based on a set of equations, that simplifies and mimics reality. Model accuracy is a big concern in control engineering. The control performance of the induction motor drive is depending on the model accuracy of the induction machine [15]. The reason for conducting this research is to investigate the model of induction motor which represents more accurately.

3.1. Three-Phase Induction Motor Dynamic D-Q Integer Order Model. A number of hypotheses are used in the modeling of the three-phase induction motor. The first hypothesis is that the magneto motive forces generated by various stator and rotor phases are distributed throughout the air gap in a sinusoidal fashion. Reaching this goal requires an adequate distribution of the windings throughout space. The machine air gap is intended to be consistently thick; notching effects and space harmonic generation are disregarded. The following hypotheses on the physical behavior of the materials are taken into account for this modeling [16].

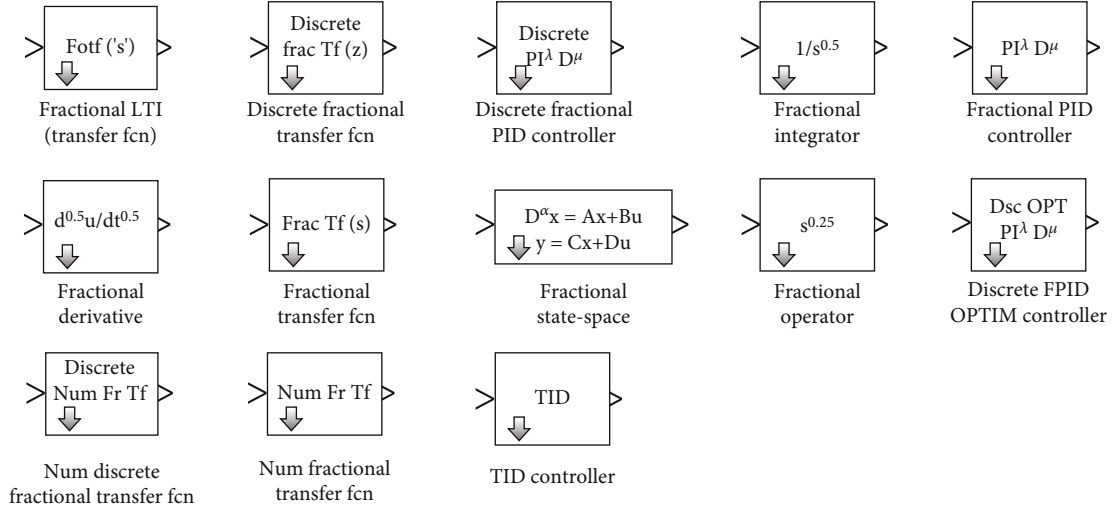


FIGURE 2: Simulink components available in FOMCON toolbox.

- (1) Skin effect is not considered
- (2) Constant motor parameters regardless of variation in temperature
- (3) Providing the magnetic fields are not saturated

The following formulas provide a mathematical formulation of a symmetrical squirrel cage-type induction motor in a synchronously rotating reference frame [17–19].

The stator voltage formulas are as follows:

$$\begin{aligned} V_{qs} &= R_s i_{qs} + \omega_e \lambda_{ds} + \frac{d}{dt} \lambda_{qs}, \\ V_{ds} &= R_s i_{ds} - \omega_e \lambda_{qs} + \frac{d}{dt} \lambda_{ds}, \\ V_{0s} &= 0 = R_s i_{0s} + \frac{d}{dt} \lambda_{0s}. \end{aligned} \quad (17)$$

The rotor voltage formulas are as follows:

$$\begin{aligned} V'_{qr} &= 0 = R'_r i'_{qr} + (\omega_e - \omega_r) \lambda'_{dr} + \frac{d}{dt} \lambda'_{qr}, \\ V'_{dr} &= 0 = R'_r i'_{dr} - (\omega_e - \omega_r) \lambda'_{qr} + \frac{d}{dt} \lambda'_{dr}, \\ V'_{0r} &= 0 = R'_r i'_{0r} + \frac{d}{dt} \lambda'_{0r}. \end{aligned} \quad (18)$$

The stator flux linkage formulas are as follows:

$$\begin{aligned} \lambda_{qs} &= L_{ls} i_{qs} + L_m (i_{qs} + i'_{qr}), \\ \lambda_{ds} &= L_{ls} i_{ds} + L_m (i_{ds} + i'_{dr}), \\ \lambda_{0s} &= 0 = L_{ls} i_{0s}. \end{aligned} \quad (19)$$

The rotor flux linkage formulas are as follows:

$$\begin{aligned} \lambda'_{qr} &= L_{lr} i'_{qr} + L_m (i_{qs} + i'_{qr}), \\ \lambda'_{dr} &= L_{lr} i'_{dr} + L_m (i_{ds} + i'_{dr}), \\ \lambda'_{0r} &= 0 = L_{lr} i'_{0r}. \end{aligned} \quad (20)$$

The mechanical formula is as follows:

$$T_e = J \frac{d\omega_r}{dt} + F\omega_r + T_L. \quad (21)$$

The electromagnetic torque formulas are as follows:

$$\begin{aligned} T_e &= \left(\frac{3}{2}\right) \left(\frac{P}{2}\right) (i_{qs} \lambda_{ds} - i_{ds} \lambda_{qs}), \\ T_e &= \left(\frac{3}{2}\right) \left(\frac{P}{2}\right) L_m (i_{qs} i'_{dr} - i_{ds} i'_{qr}), \\ T_e &= \left(\frac{3}{2}\right) \left(\frac{P}{2}\right) (\lambda'_{qr} i'_{dr} - \lambda'_{dr} i'_{qr}). \end{aligned} \quad (22)$$

Due to the symmetrical induction motor being taken into consideration in this study, the zero-sequence component becomes zero.

3.2. Three-Phase Induction Motor Dynamic D-Q Fractional Order Model. Now, we can develop a conceivable fractional order model with an undetermined differentiation order after knowing the well-known integer order model. Then, employ simulation of a fractional model for several orders of differentiation until a suitable result is reached in order to decide on the proper order of differentiation.

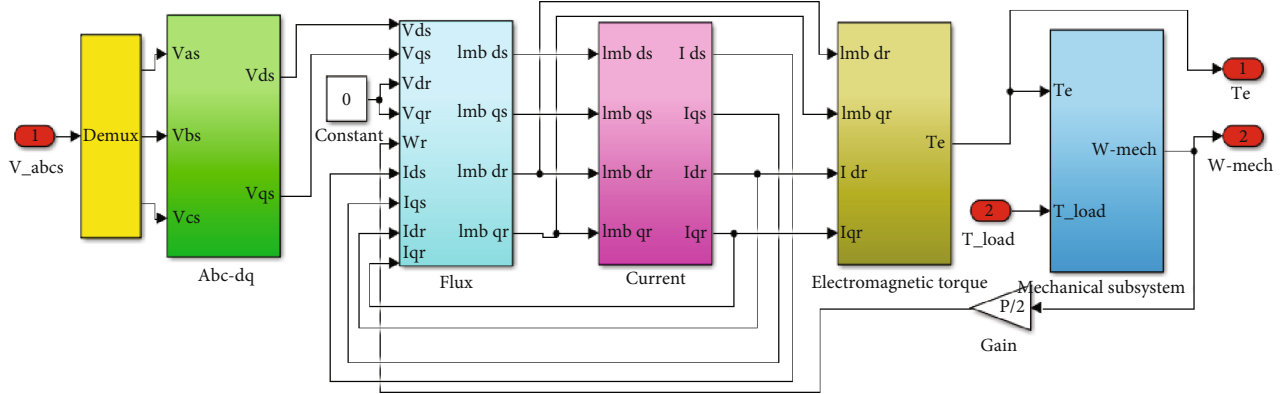


FIGURE 3: Simulink model of induction motor.

TABLE 1: Induction motor parameter values.

Quantity (unit)	Symbol	Motor I	Motor II	Motor III
Rated power (KW)	P	0.75	2.2	3
Stator resistance (ohm)	R_s	10	9.2	2.3
Stator leakage inductance (H)	L_{ls}	0.4642	0.43	0.267
Rotor resistance (ohm)	R_r	6.3	4.1	0.55
Rotor leakage inductance (H)	L_{lr}	0.4612	0.43	0.261
Mutual inductance (H)	L_m	0.4212	0.44	0.249
Frequency (Hz)	f_s	60	60	60
Pole number	p	2	4	6
Inertia (Kg.m^2)	J	0.02	0.042	0.0076
Friction factor (Nms^{-1})	B	0.2	0.0031	0.0007
Rotor angular velocity(rad/sec.)	N	373.7	185.4	122.63

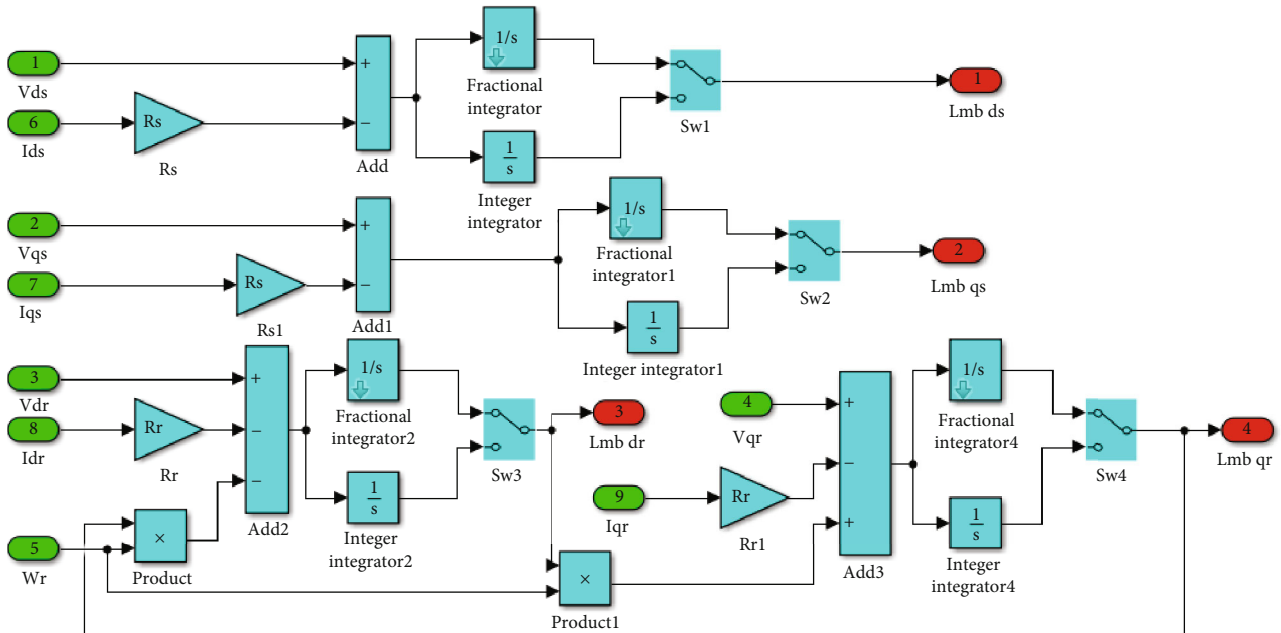
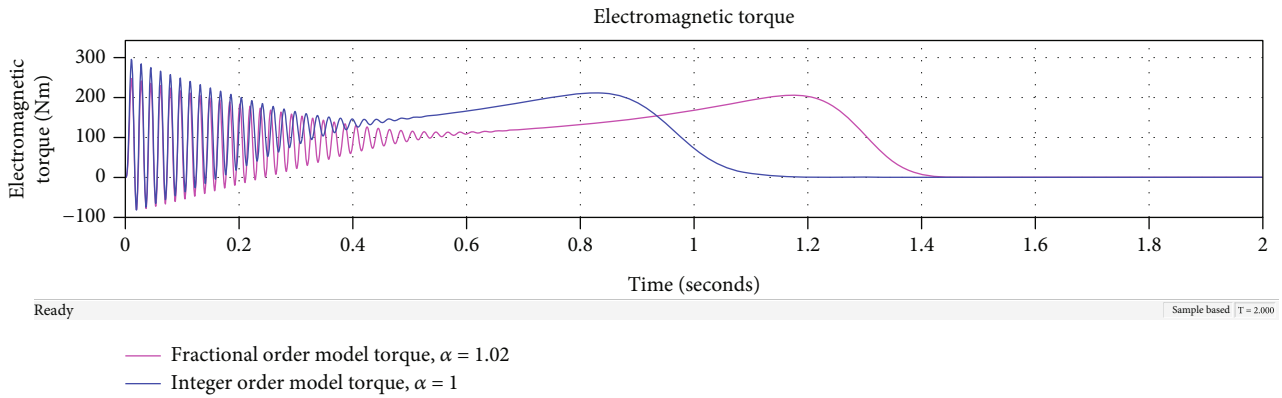
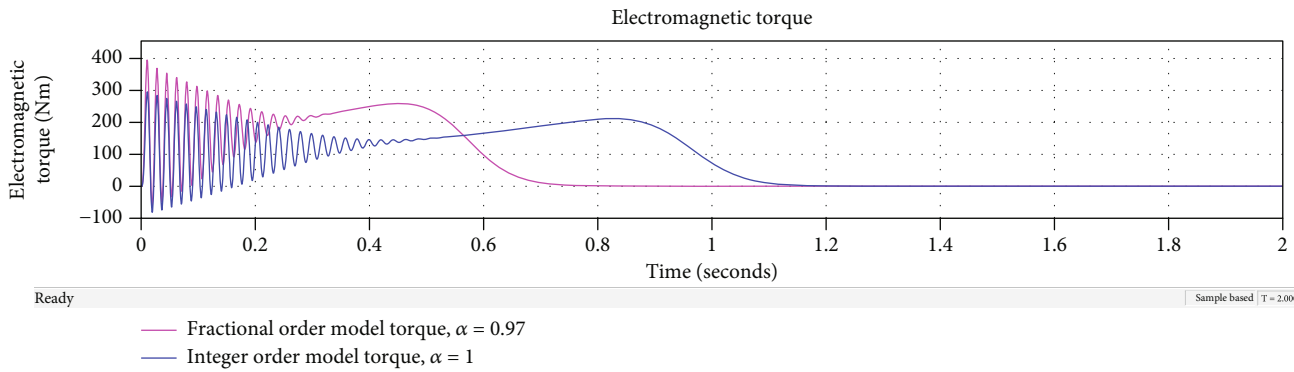


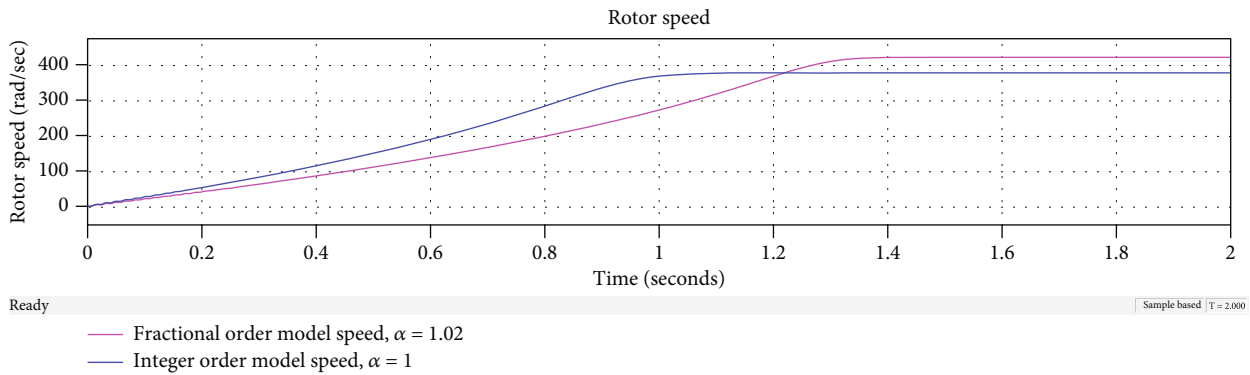
FIGURE 4: Induction motor flux block Simulink model.



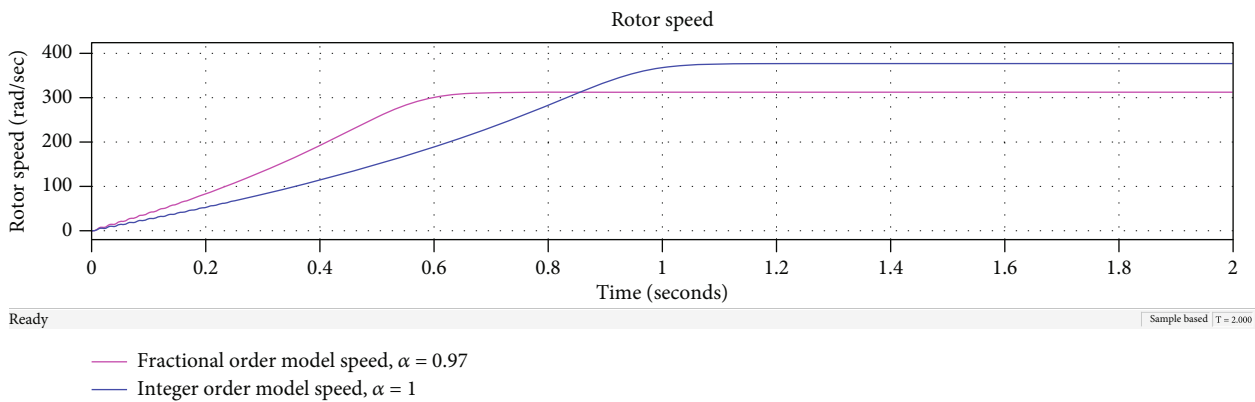
(a)



(b)

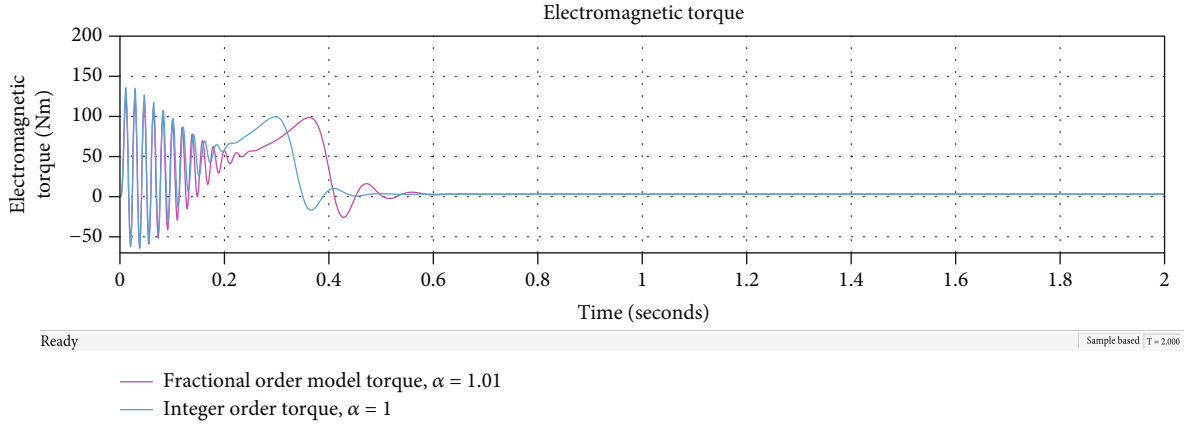


(c)

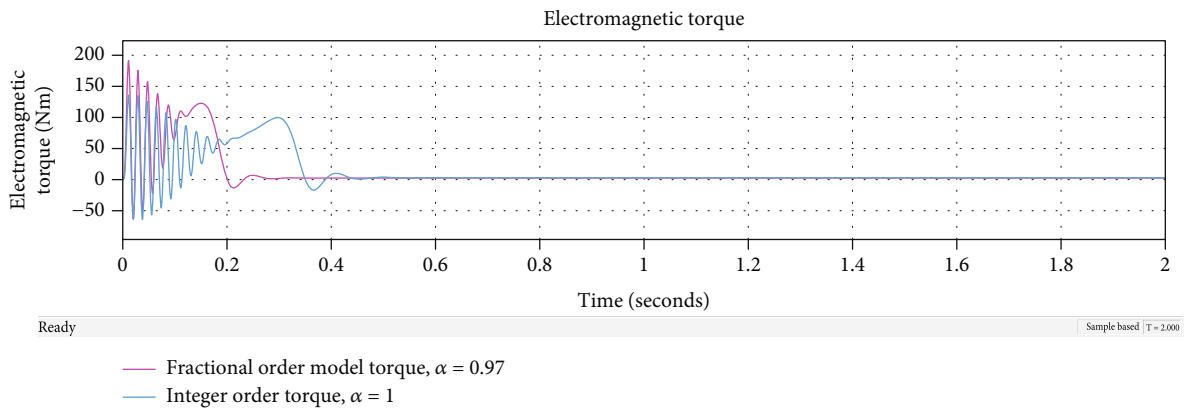


(d)

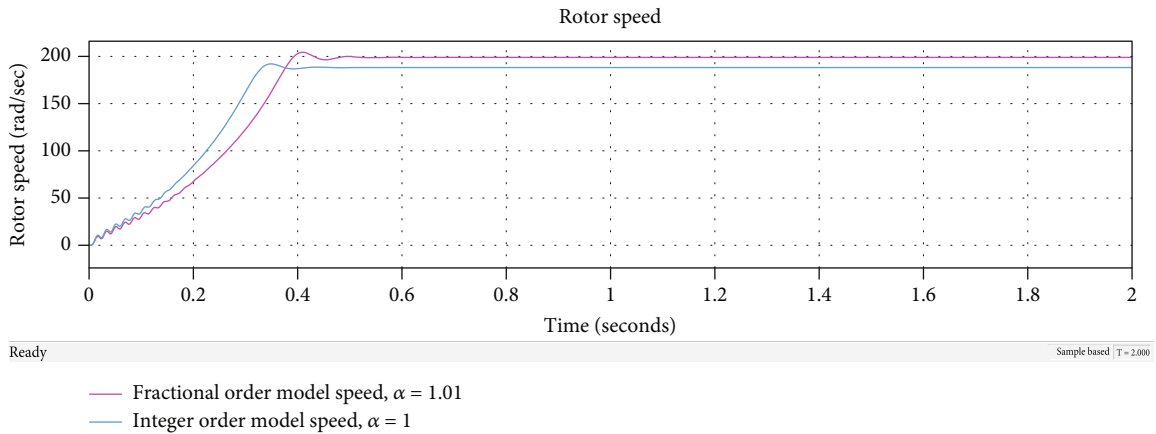
FIGURE 5: Electromagnetic torque (a ($\alpha = 1.02$ and $\alpha = 1$) and b ($\alpha = 0.97$ and $\alpha = 1$)) and speed (c ($\alpha = 1.02$ and $\alpha = 1$) and d ($\alpha = 0.97$ and $\alpha = 1$)) simulation results of motor I.



(a)



(b)



(c)

FIGURE 6: Continued.

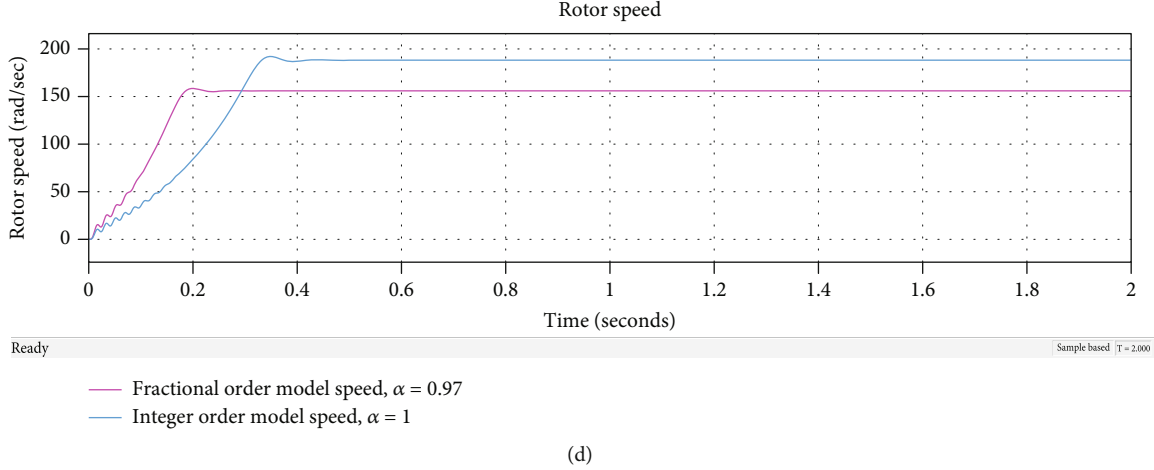


FIGURE 6: Electromagnetic torque (a ($\alpha = 1.01$ and $\alpha = 1$) and b ($\alpha = 0.97$ and $\alpha = 1$)) and speed (c ($\alpha = 1.01$ and $\alpha = 1$) and d ($\alpha = 0.97$ and $\alpha = 1$)) simulation results of motor II.

The stator voltage formulas are as follows:

$$\begin{aligned} V_{qs} &= R_s i_{qs} + \omega_e \lambda_{ds} + \frac{d^\alpha}{dt^\alpha} \lambda_{qs}, \\ V_{ds} &= R_s i_{ds} - \omega_e \lambda_{qs} + \frac{d^\alpha}{dt^\alpha} \lambda_{ds}, \\ V_{0s} &= 0 = R_s i_{0s} + \frac{d^\alpha}{dt^\alpha} \lambda_{0s}. \end{aligned} \quad (23)$$

The rotor voltage formulas are as follows:

$$\begin{aligned} V'_{qr} &= 0 = R'_r i'_{qr} + (\omega_e - \omega_r) \lambda'_{dr} + \frac{d^\alpha}{dt^\alpha} \lambda'_{qr}, \\ V'_{dr} &= 0 = R'_r i'_{dr} - (\omega_e - \omega_r) \lambda'_{qr} + \frac{d^\alpha}{dt^\alpha} \lambda'_{dr}, \\ V'_{0r} &= 0 = R'_r i'_{0r} + \frac{d^\alpha}{dt^\alpha} \lambda'_{0r}, \end{aligned} \quad (24)$$

where α is the differentiation order.

Since none of the equations in the flux linkage formula, electromagnetic torque formula, or mechanical formula contain a derivative term in motor electrical parameters, they are equivalent to the integer order model.

4. Results and Analysis

A simulation study employing various values of differentiation order (α) is conducted to prove the fractional order model of the induction motor. As seen in Figure 3, the motor is energized by the appropriate three-phase 60 Hz supply at the starting time instant ($t = 0$) to evaluate the different order of differentiation (α). It is assumed that the load torque is 0 Nm (no load).

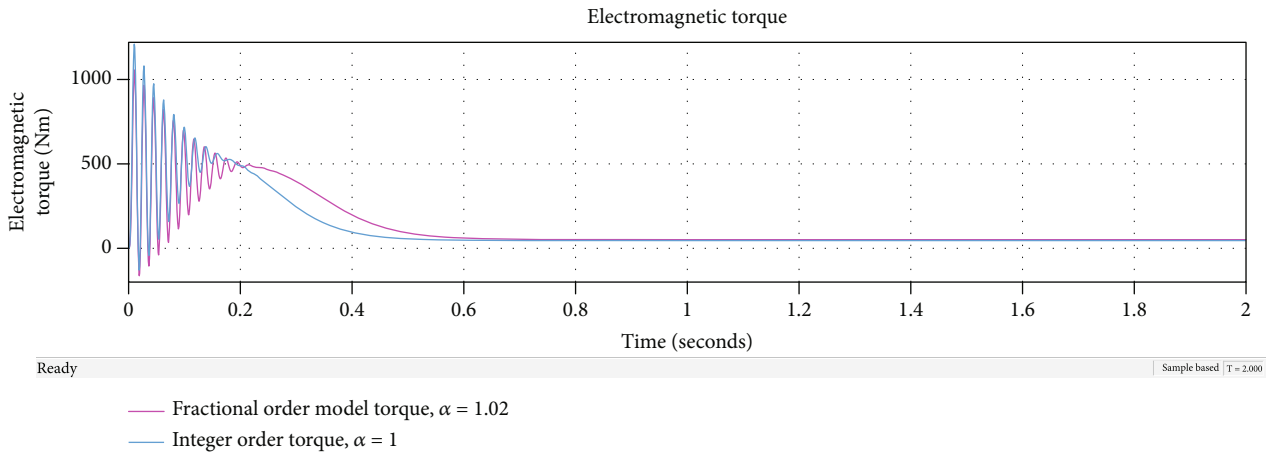
After the fractional model with an unknown order of differentiation of the induction motor has been constructed, model evaluation and order of differentiation (α) determination are required for the fractional order model. The details

of induction motors utilized for the simulation are shown in Table 1.

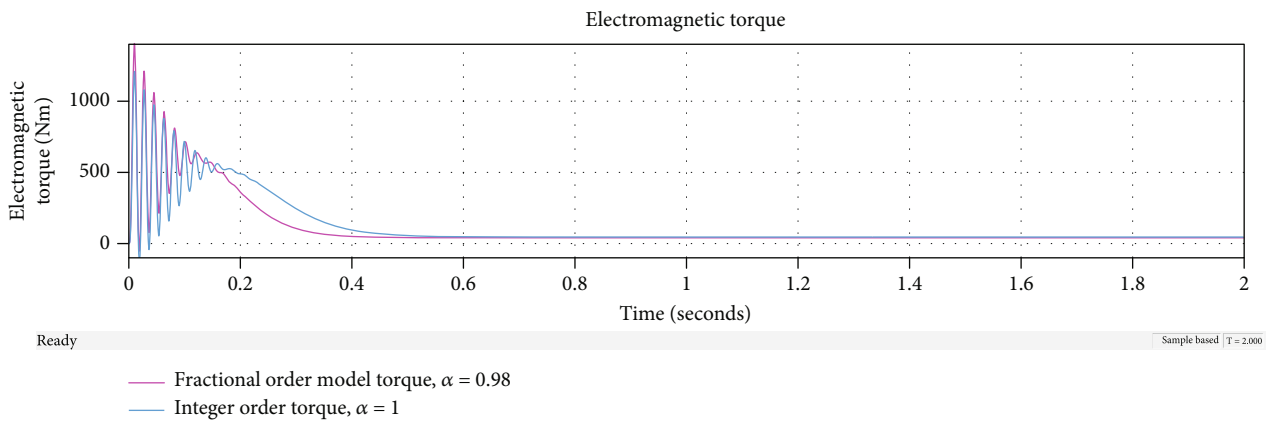
As presented in Figure 4, fractional and integer order integrators are used to implement the differential equation associated with direct and quadrature axis flux linkage.

Figures 5(a)–5(d) present the outputs of a simulation performed in MATLAB/Simulink model of the 0.75 KW squirrel cage induction motor specified as motor I in Table 1. As presented in Figure 5(a), electromagnetic torque at integration order (α) = 1.02 settles to its near-zero value after the electromagnetic torque of integer order ($\alpha = 1$) result settles. When we come to Figure 5(b) at $\alpha = 0.97$, the electromagnetic torque settles before the integer-order model electromagnetic torque. Based on the results, as the integration order increases, the electromagnetic torque becomes slower to settle to its final value. Similarly, as presented in Figure 5(c) at $\alpha = 1.02$, the rotor speed settles its final value at 1.384 sec. and the final value becomes 420.79 rad/sec. Additionally, at $\alpha = 1$, the rotor speed settles its final value at 1.1 sec. and the final value becomes 376.93 rad/sec. As shown in Figure 5(d) at $\alpha = 0.97$, the rotor speed settles its final value at 0.642 sec. and the final value becomes 312.42 rad/sec. The above results show that as the integration order increases, the slower the no-load motor rotor speed settles to some constant speed.

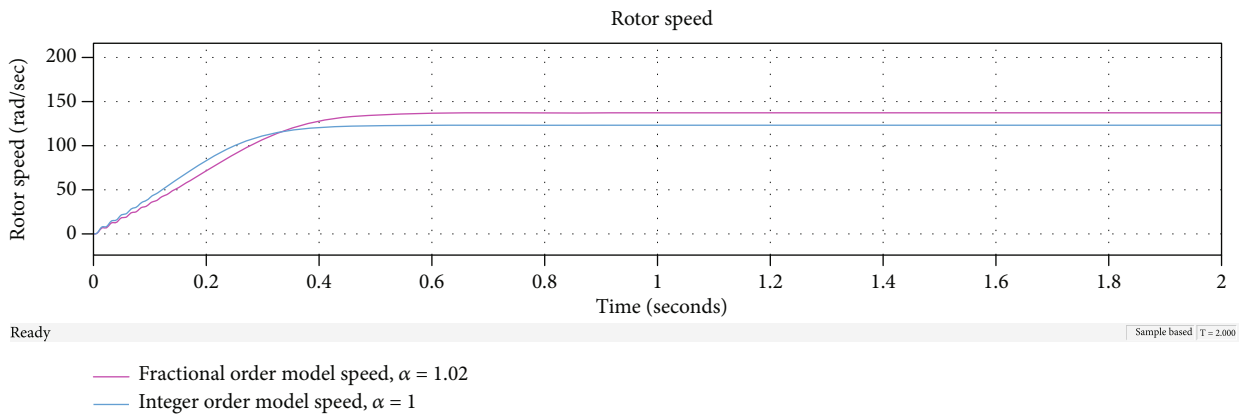
The outputs of a MATLAB simulation utilizing the Simulink model of the 2.2 KW squirrel cage induction motor designated as motor II in Table 1 are displayed in Figures 6(a)–6(d). The electromagnetic torque at $\alpha = 1.01$ settles to a value that is quite close to zero after the electromagnetic torque of integer order ($\alpha = 1$) result settles, as presented in Figure 6(a). The electromagnetic torque settles ahead of the integer-order model electromagnetic torque at $\alpha = 0.97$, as seen in Figure 6(b). According to the findings, the electromagnetic torque takes longer to reach its final value as the integration order increases. Similar to this, in Figure 6(c) at $\alpha = 1.01$, the rotor speed settles its final value at 0.56 sec. and the final value becomes 198.8 rad/sec. Additionally, at $\alpha = 1$, the rotor speed settles its final value at 0.451 sec. and the final value becomes 188.3 rad/sec. As



(a)



(b)



(c)

FIGURE 7: Continued.

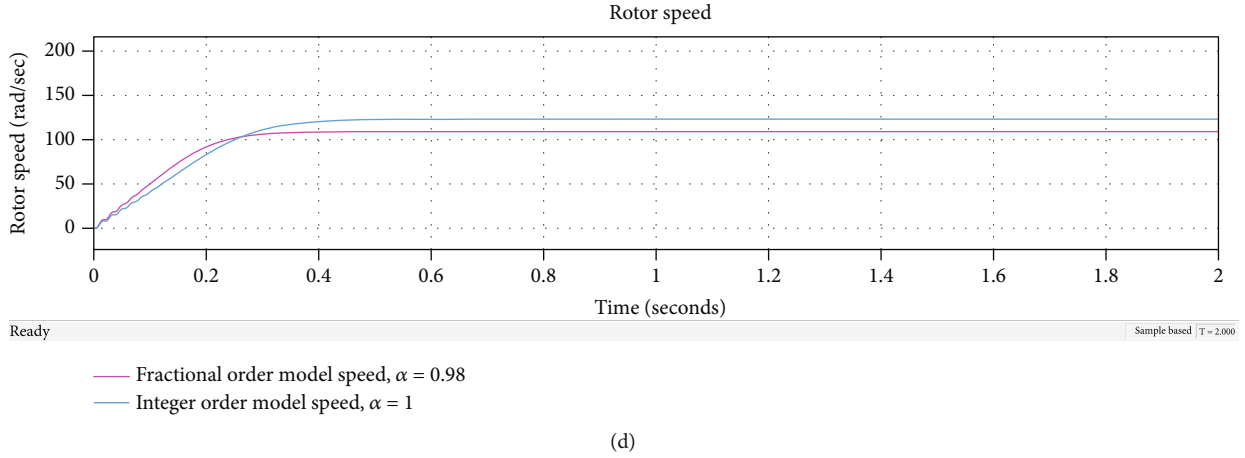


FIGURE 7: Electromagnetic torque (a ($\alpha = 1.02$ and $\alpha = 1$) and b ($\alpha = 0.98$ and $\alpha = 1$)) and speed (c ($\alpha = 1.02$ and $\alpha = 1$) and d ($\alpha = 0.98$ and $\alpha = 1$)) simulation results of motor III.

TABLE 2: Criteria of simulation results at different order of differentiation (α).

Motor	Differentiation order	Maximum torque (Nm)	Electromagnetic torque settling time (sec.)	Settled torque (Nm)	Speed settling time (sec.)	Settled speed (rad/sec.)	Calculated synchronous speed (rad/sec.)
I	1.02	247.7	1.44	0.421	1.384	420.79	376.99
	1	295.5	1.12	0.375	1.10	376.93	
	0.97	395.2	0.72	0.312	0.642	312.42	
II	1.01	123.8	0.64	3.24	0.56	198.8	188.5
	1	135.7	0.57	3.065	0.451	188.3	
	0.97	191.3	0.32	2.54	0.28	155.8	
III	1.02	603.1	0.76	51.96	0.711	139.5	125.66
	1	724.3	0.54	46.43	0.48	124.8	
	0.98	887.5	0.393	41.06	0.35	110.2	

shown in Figure 6(d) at $\alpha = 0.97$, the rotor speed settles its final value at 0.28 sec. and the final value becomes 155.8 rad/sec. The above results show that the no-load motor rotor speed settles to a steady speed more slowly as the integration order increases.

The outcomes of a MATLAB simulation utilizing the Simulink model of the 3 KW squirrel cage induction motor listed in Table 1 as motor III are presented in Figures 7(a)–7(d). As presented in Figure 7(a), electromagnetic torque at integration order (α) = 1.02 settles to its near-zero value after the electromagnetic torque of integer order ($\alpha = 1$) result settles. Figure 7(b) at $\alpha = 0.98$ shows that the electromagnetic torque settles before the integer-order model electromagnetic torque. The results show that the electromagnetic torque takes longer to reach its final value as the order of integration increases. In Figure 7(c) at $\alpha = 1.02$, the rotor speed settles its final value at 0.711 sec. and the final value becomes 139.5 rad/sec. Additionally, at $\alpha = 1$, the rotor speed settles its final value at 0.48 sec. and the final value becomes 124.8 rad/sec. As shown in Figure 7(d) at $\alpha = 0.98$, the rotor speed settles its final value at 0.35 sec. and the final value becomes 110.2 rad/sec. The above results show that as the integration order increases, the slower the no-load motor rotor speed settles to some constant speed.

A squirrel cage induction motor has an electromagnetic torque that is very small or almost nil when there is no load. This is due to the fact that the rotor of a squirrel cage induction motor functions according to the induction principle, in which the rotor currents are induced by the revolving magnetic field generated by the stator windings.

The revolving sinusoidal flux is generated in the air gap at a speed determined by Equation (25) when excited by a sinusoidal source delivered to the stator's windings.

$$N_s = \frac{120f_s}{P}, \quad (25)$$

where N_s is the synchronous speed expressed in rpm, f_s is the applied excitation's frequency in Hz, and P represents the number of stator poles.

The best value of α is chosen using a variety of criteria. The value determined by Equation (25) does not match the speed response of fractional order models when there is no load.

As can be observed from Table 2, maximum torque falls as the order of integration (α) rises, whereas the speed at no-load rises and settling time for speed and torque rises.

Equation (25) calculates the synchronous speed, which is almost identical to the simulation output at an integer order of $\alpha = 1$. As a result, an integer order model is the induction motor's optimum model.

5. Conclusion

To study the fractional order model of induction motor, evaluation of the results of speed and torque simulations without load with various values of differentiation order (α) below and above one has been performed. Three various induction motors with various parameters have been taken into consideration. FOMCON toolbox was incorporated into MATLAB and utilized for simulation with regard to fractional orders. The optimal differential order (α) is chosen based on a variety of evaluation criteria, including peak torque, speed and torque settling times, and final speed and torque values under no load conditions. The integer order model is the best representation of the induction motor based on the examination of simulation results.

Data Availability

The author declares that all data presented in this work were generated during the course of the work and any other source has been appropriately referenced within the manuscript.

Conflicts of Interest

The author declares that they have no conflicts of interest.

References

- [1] A. Tepljakov and T. T. Kirjastus, *Fractional-Order Modeling and Control of Dynamic Systems*, TUT Press, 2015.
- [2] J. Morsali, K. Zare, and M. Tarafdar Hagh, "Applying fractional order PID to design TCSC-based damping controller in coordination with automatic generation control of interconnected multi-source power system," *Engineering Science and Technology, an International Journal*, vol. 20, no. 1, pp. 1–17, 2017.
- [3] A. Tepljakov, "FOMCON: fractional-order modeling and control toolbox," in *Fractional-Order Modeling and Control of Dynamic Systems*, pp. 107–129, Springer, 2017.
- [4] H. Deng and Q. Wang, "Dynamics and synchronization of memristor-based fractional-order system," *International Journal of Modern Nonlinear Theory and Application*, vol. 2, no. 4, pp. 223–227, 2013.
- [5] A. Tepljakov, "Fractional-order calculus based identification and control of linear dynamic systems," *Tallinn University of Technology*, 2011.
- [6] F. Martínez González and M. K. A. Kaabar, *Applied Mathematics and Fractional Calculus* <http://www.mdpi.com/journal/symmetry>.
- [7] Zhuo, "UC Merced UC Merced electronic theses and dissertations title fractional order modeling and control of multi-input-multi-output processes," <https://escholarship.org/uc/item/49x9x167>.
- [8] A. Atangana and A. Secer, "A note on fractional order derivatives and table of fractional derivatives of some special functions," *Abstract and Applied Analysis*, vol. 2013, Article ID 279681, 8 pages, 2013.
- [9] M. F. Khan, M. R. Khan, and A. Iqbal, "Effects of induction machine parameters on its performance as a standalone self excited induction generator," *Energy Reports*, vol. 8, pp. 2302–2313, 2022.
- [10] A. M. de Almeida, M. K. Lenzi, and E. K. Lenzi, "A survey of fractional order calculus applications of multiple-input, multiple-output (MIMO) process control," *Fractal and Fractional*, vol. 4, no. 2, p. 22, 2020.
- [11] D. Xue, "FOTF toolbox for fractional-order control systems," in *Applications in Control*, pp. 237–266, De Gruyter, 2019.
- [12] M. A. A. Ghany, M. E. Bahgat, W. M. Refaey, and S. Sharaf, "Type-2 fuzzy self-tuning of modified fractional-order PID based on Takagi–Sugeno method," *Journal of Electrical Systems and Information Technology*, vol. 7, no. 1, p. 2, 2020.
- [13] D. Valério and J. S. Da Costa, "Ninteger: a non-integer control toolbox for Matlab," in *Proceedings of Fractional Differentiation and its Applications*, Bordeaux, 2004.
- [14] R. Malti and S. Victor, "CRONE toolbox for system identification using fractional differentiation models," in *IFAC-PapersOnLine*, pp. 769–774, Elsevier B.V., 2015.
- [15] Y. Li, "Mathematical modeling methods and their application in the analysis of complex signal systems," *Advances in Mathematical Physics*, vol. 2022, Article ID 1816814, 10 pages, 2022.
- [16] B. Robyns, B. Francois, P. Degobert et al., "Vector control of induction machines," *Power Systems*, vol. 57, 2012.
- [17] M. S. Bhagyashree and R. Adappa, "Modelling and simulation of an induction machine," *International Journal of Innovative Research in Electrical, Electronics, Instrumentation and Control Engineering*, vol. 4, no. 2, pp. 119–123, 2016.
- [18] P. Dorji and B. Subba, "D-Q mathematical modelling and simulation of three-phase induction motor for electrical fault analysis," *International Advanced Research Journal in Science, Engineering and Technology*, vol. 7, no. 9, pp. 38–46, 2020.
- [19] R. Rahmatullah, N. F. O. Serteller, and V. Topuz, "Modeling and simulation of faulty induction motor in DQ reference frame using MATLAB/SIMULINK with MATLAB/GUIDE for educational purpose," *International Journal of Education and Information Technologies*, vol. 17, pp. 7–20, 2023.